



## Photoluminescence from CdS Quantum Dots in Silica Gel

NICOLÁS DE LA ROSA-FOX\*

*Departamento Física Materia Condensada, Facultad de Ciencias, Universidad de Cádiz,  
11510 Puerto Real (Cádiz), Spain*

nicolas.rosafox@uca.es

MANUEL PIÑERO

*Departamento Física Aplicada, CASEM, Universidad de Cádiz, 11510 Puerto Real (Cádiz), Spain*

ROCÍO LITRÁN AND LUIS ESQUIVIAS

*Departamento Física Materia Condensada, Facultad de Ciencias, Universidad de Cádiz,  
11510 Puerto Real (Cádiz), Spain*

**Abstract.** CdS semiconductor nanocrystals were grown as quantum dots (QDs) inside a silica matrix obtained by the sol-gel method and assisted in the mother liquid by high power ultrasounds. Small-angle neutron scattering (SANS) accounts for a 3.6 nm crystal size homogeneously distributed. Optical excitation from the third harmonic of a Nd:YAG ns laser was focused on the sample to study the photoluminescence (PL) at room temperature. The PL spectrum shows radiative process from intrinsic transitions and a broad band corresponding to the traps. Variable stripe length (VSL) method was used to measure the optical gain spectra by the growth of the amplified luminescence. A broad optical gain spectrum produced by the biexciton-exciton transitions revealing the stimulated emission from the CdS QDs. It is also observed a red-shift of the PL emission crystal size-dependent.

**Keywords:** sonogel, CdS nanocrystals, photoluminescence, SANS, optical gain

### 1. Introduction

Semiconductors QDs embedded in a dielectric matrix show interesting optical non-linear properties due to the quantum confined excitons [1, 2]. Crystal size and its volume fraction play a fundamental role in the electronic structure of the QD [3]. In this way, the creation of one electron-hole pair (1EHP-exciton) or two (2EHP-biexciton) bounded, provide the Coulomb potential screening scenario that provoke the optical non-linearity in these systems. This new optical behaviour is induced by the drastic modification of the electronic structure in the nanocrystal, giving place to a discrete single-particle states with higher energy

gaps. An interesting property of the biexciton emission is the possibility to obtain large optical gain, in contrast to the direct free exciton decay where substantial optical gain is not possible because of the reabsorption. A broad gain spectrum will appear instead of sharp discrete lines as a new typical feature in these zero-dimensional semiconductors [1]. The optical gain in these systems proceeds from the biexciton-exciton transition that produces the superlineary growth of the integrated luminescence. Also, a red-shift of the PL relative to the absorption, as other specific characteristic of QDs, is crystal size-dependent as the result of the confinement effects [4, 5].

The sol-gel method can be used to improve the crystal growth by precipitation from solution inside a silica gel matrix [6, 7]. This processing method has been

\*To whom all correspondence should be addressed.

demonstrated the possibility to upgrade some critical parameters, such as: higher dot density, smaller dot size and better distribution and homogeneity, the optical quality of the matrix, a performed matrix microporosity and the passivated crystal surface as other improvements in these materials [8, 9].

We introduce some variation in the processing as the use of ultrasounds to promote the chemical reactions and the use of Formamide as a chemical additive to control the gel aging process [10]. We report using the VSL method [11] the optical gain spectrum. We resolve the two PL bands of colloidal QDs in gels at room temperature.

## 2. Experimental

The sol-gel process uses a TMOS:H<sub>2</sub>O (pH 1):Formamide mixture in a molar ratio of 1:4:7. At this step the liquid is submitted to a 320 J cm<sup>-3</sup> ultrasounds energy, provoking a faster reaction of the alkoxide. Cadmium acetate is added to the solution as source of the Cd<sup>+2</sup> ions. By flowing H<sub>2</sub>S at 150°C through the casting gel permits the nucleation and growth of the CdS crystals. Yellow coloured samples are heat-treated at 500°C in order to stabilize the matrix and to prevent any further crystal growth. The CdSX sample code refers to X = 1, 3 and 10 wt% of CdS, considering a total CdO crystal transformation in CdS, after H<sub>2</sub>S gas diffusion. The CdO code refers to the undoped matrix prior the H<sub>2</sub>S gas diffusion.

SANS measurements were carried out on V4 workstation at the Berlin Neutron Scattering Centre facility in the Hahn-Meitner Institut (Berlin, Germany) [12]. Scattering data were obtained using sample-detector distances of 1, 4 and 16 m, covering a  $q$ -range of 0.036 to 3.6 nm<sup>-1</sup> by selecting a neutron wavelength of 0.6 nm.

PL intensities were measured by using the third harmonic (3.49 eV) of a pulsed Nd:YAG laser (6 ns pulse at 10 Hz repetition rate). By means a cylindrical lens the laser beam is focused on the edge of the sample to form a narrow rectangular stripe (50 μm to 2 mm long and 20 μm wide) [13, 14]. The amplified luminescence (AL) at right angles in the direction of the stripe is collected for different stripe lengths. The laser spot on the sample was carefully positioned to avoid the scattering from the edge roughness of the gel. In all cases the PL measurements were performed at atmospheric pressure in air at room temperature.

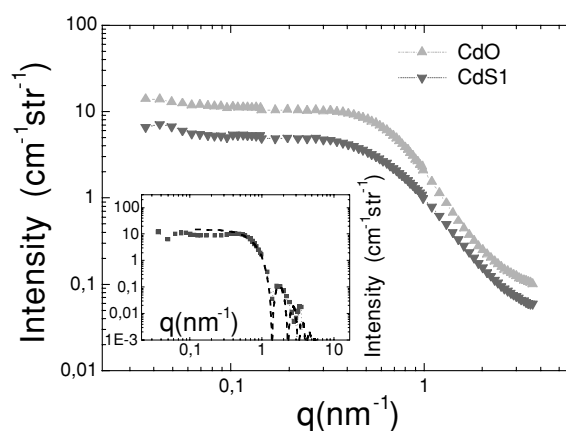


Figure 1. SANS intensity curves for the outlined samples ( $q = \frac{4\pi \sin \theta}{\lambda}$ , where  $2\theta$  is the scattering angle and  $\lambda$  the neutron wavelength). Inset, intensity curve for a sphere of 3.6 nm (dashed) and the resulting curve after Eq. (1) (solid squares).

## 3. Results and Discussion

Figure 1 shows the scattering intensities, before (CdO) and after (CdS1) H<sub>2</sub>S diffusion. The higher intensity for the CdO sample coming from the large scattering length density (SLD) value of CdO crystals in relation to the CdS one. SLD difference was taken between the corresponding to the crystal and a 60% SiO<sub>2</sub> matrix of relative mass density. This difference in SLD will permit to isolate the crystal signal, from the fact that the origin of scattered neutrons lies in the mismatch between the scattering length density of the silica matrix network and the nanocrystals by fitting the relationship:

$$I(\text{SiO}_2/\text{CdO}) - KI(\text{SiO}_2/\text{CdS}) = I_0 \exp\left(-\frac{q^2 R_g^2}{3}\right) \quad (1)$$

in order to obtain a  $K$  value to get back the best Guinier region, where  $R_g$  is the gravity centre of the scatters. Considering a similar porosity in both samples and a total CdO crystal transformation in CdS after H<sub>2</sub>S gas diffusion, the intensity of the Eq. (1) must correspond to the difference in contrast between the CdO and the CdS crystals. The inset in the Fig. 1 shows the resulting curve compared to the scattering from a sphere of 3.6 nm radius. As the  $R_g$  calculated value of 2.8 nm corresponds to an sphere of 3.6 nm, it permits to consider the CdS crystals spherical shaped homogeneously distributed inside the matrix.

The optical absorption band is blue-shifted from the bulk CdS band gap at 2.53 eV, as it is shown on the

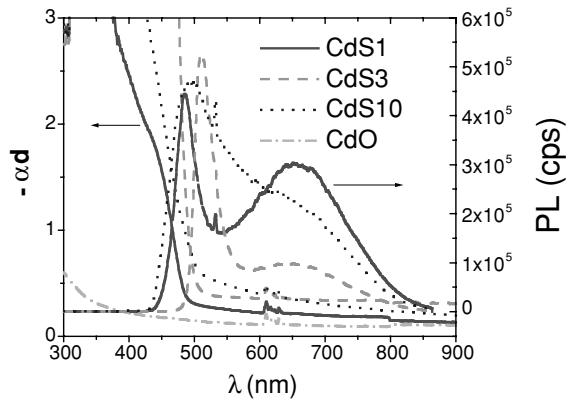


Figure 2. Optical density (left axis) of the outlined samples together the CdO one included as transparent reference (bottom). Photoluminescence (PL) signal (right axis) of the same samples.

Fig. 2 (left axis), revealing the quantum confinement effects. In this way, from the effective mass approximation (EMA) model ( $\Delta E \propto R^{-2}$ )<sup>1</sup> a CdS crystal of 2.6 nm radius should be responsible of the quantum confinement effects in the CdS1 sample, in agreement with the Guinier radius calculated from SANS. Table 1 show the optical and structural parameters for the studied samples. In agreement with the EMA model the blue-shift is crystal size-dependent.

Two bands can be observed on the PL signals in Fig. 2 (right axis). The highest-energy one is related to the intrinsic recombination mechanism. It is also possible weakly allowed transitions for dots with  $R \cong a_B = 3.2$  nm in CdS, because kinetic energy terms dominate against Coulomb effects and produces the observed inhomogeneous line broadening. On the other hand, the lowest-energy one being attributed to the recombination of trapped carriers.

It is also observed, in the Fig. 2, a red-shift of the PL emission relative to the absorption band, from the values on Table 1 it can be concluded that it is crystal size-dependent, the red-shift increases as the particle

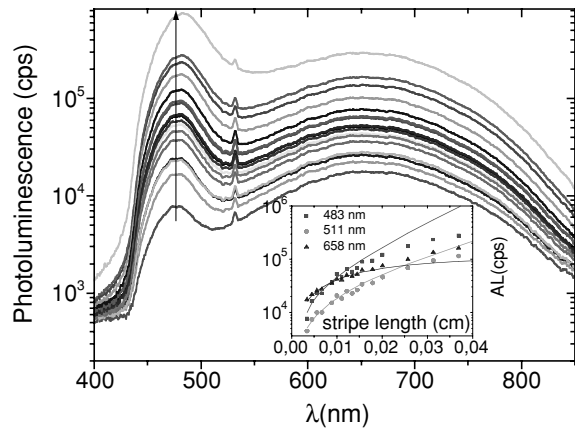


Figure 3. PL yield of the CdS1 sample as a function of the experimental stripe length (bottom to top), the arrow guide for the maximum red-shift and the small peak at 512 nm is the residual of the laser line. Inset, luminescence for some wavelengths (points) and the corresponding result of the fitting of Eq. (2) (line).

size decreases. The origin of this effect seems to be related with a crystal lattice distortion after the transformation of the CdO (cubic) in CdS (hexagonal) at 150°C provoking compressive strains. This fact influences the intrinsic band due to the S ions vacancies acting as potential hole traps. The observable differences in the spectra also inform about the crystal surface traps, CdS3 sample seems to have lower traps states than CdS1. However, CdS10 sample shows an overlapping of both bands indicating a higher lattice distortion. In the light of these size-dependent effects (blue and red-shift) the no correlation between crystal size and CdS content must be attributed to the slight difference of the silica network pore structure which affects the H<sub>2</sub>S gas diffusion.

Figure 3 shows the growth of the PL signal for the CdS1 sample. In these experimental conditions the PL yield along the focus axis is related with the optical gain by the relationship [11]:  $I_{AL} = \frac{I_{SP}}{g} (e^{gL} - 1)$ , where  $I_{AL}$  and  $I_{SP}$  are the amplified and spontaneous

Table 1. Optical and structural experimental values of the CdS-SiO<sub>2</sub> composites.

Sample	Blue-shift (meV)	Red-shift (meV)	<i>a</i> (nm) (EMA)	Raman <sup>a</sup> (nm)	SANS (nm)
CdS1	388	356	2.6	2.2	2.8
CdS3	48	151	7.1	3.2	X
CdS10	207	222	3.4	2.8	X

The contents of CdS are 1, 3 and 10 wt% relative to the Cds-SiO<sub>2</sub> composite, called CdS1, CdS3 and CdS10, respectively.

<sup>a</sup>Source: R. Litran, R. Alcántara, E. Blanco, and M. Ramirez-del-Solar, J. Sol-Gel Sci. Tech. **8**, 275 (1997).

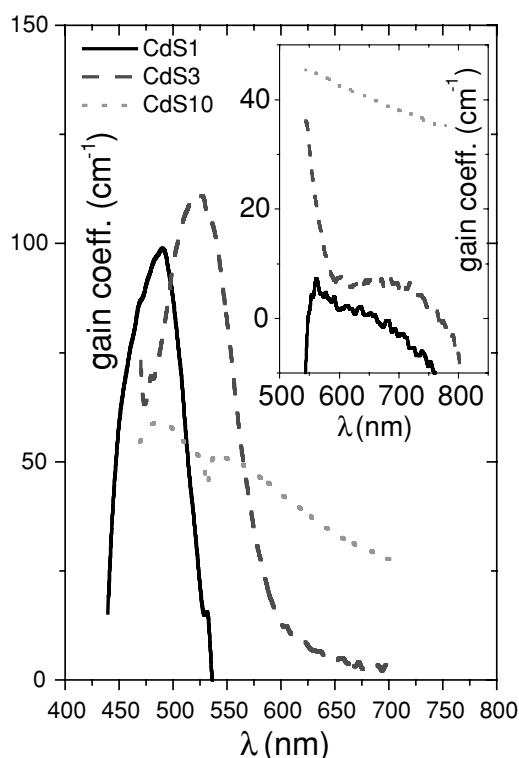


Figure 4. Optical gain spectra for the filtered intrinsic band (Schott BG-14) of the studied samples. Inset, gain spectra for the filtered traps band (Schott OG-550).

emission, respectively. The net gain coefficient is  $g$  and the experimental variable stripe length is  $L$ . By fitting the experimental data to the above equation,  $g$  and  $I_{SP}$  can be calculated as it shown in the inset of Fig. 3 for some wavelengths. As can be observed the gain saturation limits the stripe length domain for which the amplification grows exponentially. In this case (483 and 511 nm), saturation effects seem to be produced for approximately  $gL > 3$ , faster than in bulk semiconductors ( $gL > 5$ ) but similar to others semiconductors QDs ( $gL > 2$ ) [14]. This effect is also observable as a weakly red-shift on the PL maximum.

The PL yield grows in a superlinear fashion for the intrinsic band, but not at all for the traps one, as can be seen on Fig. 4. The gain is spectrally broad with a steeper decrease on the high-energy side and a long tail stretching to lower energies. As can be seen the CdS1 and CdS3 samples have similar spectra, which follow similar feature than the PL one (Fig. 3). This fact indicates the passivated crystal surface of the CdS3 sample as contrasted with the crystal size difference with the CdS1 (see Table 1). On the contrary,

CdS10 with similar crystal size than CdS1 shows a decline in the gain spectrum due to a higher surface defects.

#### 4. Conclusions

Sol-gel method assisted by high power ultrasounds permits the obtention of CdS QDs with narrow size distribution in CdS1 sample. Blue-shift confirm the confinement effects. The red-shift of the PL emission is crystal size-dependent coming from crystalline lattice distortions. Nanocrystals of the CdS3 sample are in the limit of the confinement regime, but having better passivated surfaces that produce optical gain. On the contrary, the crystal surface defects of the CdS10 sample with crystal size close to the confinement regime, produce a decline in the gain spectrum. The optical gain reveals the stimulated emission from the CdS QDs.

#### Acknowledgments

SANS measurements in the HMI (Berlin, Germany) was supported by the TMR/LSF access program (ERBFMGE CT950060) of the European Commission. Financial support from Spanish Government (MAT98-0798) and Junta de Andalucía (TEP-0115). N.R.F. acknowledge to Prof. Peyghambarian for the optical facilities in the Optical Science Center of the University of Arizona (Tucson, USA).

#### References

1. U. Woggon, in *Optical Properties of Semiconductors Quantum Dots*, Springer Tracts Modern Physics, Vol. 136 (Springer, Berlin, 1997).
2. S.C. Moss, D. Ila, H.W.H. Lee, and D.J. Norris (Eds.), *Semiconductor Quantum Dots*, Mat. Res. Soc. Symp. Proc., Vol. 571, (PA, USA, 2000).
3. N. Peyghambarian, S.W. Koch, and A. Mysyrowicz, in *Introduction to Semiconductors Optics* (Prentice-Hall, New Jersey, 1993).
4. H.W.H. Lee, C.A. Smith, V.J. Leppert, and S.H. Risbud, in *Semiconductor Quantum Dots* Mat. Res. Soc. Symp. Proc., Vol. 571 p. 259.
5. H. Fu and A. Zunger, *Phys. Rev. B* **56**, 1496 (1997).
6. E. Blanco, L. Esquivias, R. Litrán, M. Piñero, M. Ramírez-del-Solar, and N. de la Rosa-Fox, *Appl. Organometal. Chem.* **13**, 399 (1999).
7. R. Erce-Montilla, M. Piñero, A. Santos, N. Rosa-Fox, and L. Esquivias, *J. Mater. Res.* **16**, 2572 (2001).

8. M. Guglielmi, A. Martucci, E. Menegazzo, G.C. Righini, S. Pelli, J. Fick, and Y.G. Vitrant, *J. Sol-Gel Sci. Techn.* **8**, 1017 (1997).
9. A. Martucci, J. Fick, J. Scell, G. Battaglin, and M. Guglielmi, *J. Appl. Phys.* **86**, 79 (1999).
10. A. Craievich, N. de la Rosa-Fox, E. Blanco, M. Piñero, M. Ramírez-del-Solar, and L. Esquivias, *NanoStruct. Mat.* **5**, 363 (1995).
11. K.L. Shaklee, R.E. Nahory, and R.F. Leheny, *J. Lumin.* **7**, 284 (1973).
12. E. Hoinkis, *Langmuir* **12**, 4299 (1996).
13. J. Butty, Y.Z. Hu, N. Peyghambarian, Y.H. Kao, and J.D. Mackenzie, *Appl. Phys. Lett.* **67**, 2672 (1996).
14. J. Butty, N. Peyghambarian, Y.H. Kao, and J.D. Mackenzie, *Appl. Phys. Lett.* **69**, 3224 (1996).